Global-Local FE Simulation of a Plate LVI Test

F. Caputo, G. Lamanna, A. De Luca[1], R. Borrelli and S. Franchitti[2]

Abstract: The aim of the proposed research activity is to investigate on the structural behaviour of laminated composite plates, in order to develop numerical models able to describe their "damage resistance" under low velocity impacts. To achieve these results it is necessary to provide understanding of and ultimately predict the initiation and the progression mechanisms of damage. Since analytical closed-form methods are unable to describe simultaneously different failure modes and experimental testing can give indications only for specific cases, not generally applicable, it is necessary to improve numerical techniques, which on the base of opportunely selected and calibrated models are able to describe and forecast the damage growth behaviour. A global/local modelling approach has been used to develop explicit finite element analyses of the impact event, including damage initiation and propagation. For validation purpose, numerical results are compared with data from two series of experimental impact tests, by considering impact energy values of 50 J and 100 J, respectively.

Keywords: Composite, Low Velocity Impact, Finite Element Analysis, Damage.

1   Introduction

Studies on delaminations and on other damage mechanisms involved in a composite structure failure have been conducted separately. Indeed, in literature, several works can be found which are dedicated separately to delamination and intra-laminar damages; however these phenomena are seldom analyzed together by discussing how the interferences between the different damage mechanisms can influence their evolution under various loading conditions. The delamination damages have been extensively investigated both experimentally and numerically and, when applicable, analytical models have been developed. A first analytical model has been developed by Chai, Babcock and Knauss (1981) where, based on the "thin film" approximation, a prediction of the strain needed to cause delamination buckling is

---

[1] The Second University of Naples, DIII, Italy.
[2] Italian Aerospace Research Center – C.I.R.A. S.p.A., Capua, Italy.

given together with an approximate evaluation of the energy release rate for the delamination growth initiation in a composite laminate under compressive load. Further analytical works have been made by Kardomates and Schmueser (1988) who investigated the buckling and post buckling behavior of homogeneous orthotropic linear elastic laminates with a through-width delamination taking into account also transverse shear effects. Earlier numerical studies have been carried out by Whitcomb (1986), where 2-dimensional models have been proposed. 3-dimensional numerical approaches are presented by Fei, and Yin (1984). All the cited models, even if capable to provide a realistic stress distribution in the delamination area, are not able to simulate the growth of delaminations. In Armentani, Caputo, Esposito and Godono (2004), Riccio, Caputo and Tessitore (2013), Riccio, Zarrelli and Caputo (2013), Nilsson, Thesken, Sindelar, Giannakopoulos and Storakers (1993); Caputo, Esposito, Perugini and Santoro (2002), 2D and 3D models are presented, with the aim to describe the delamination growth by adopting the Virtual Crack Closure Technique to evaluate the Energy Release Rate. Considerable either numerical or experimental studies have been also devoted to the understanding of the damage onset and propagation in composite structures in terms of matrix and fiber breakage [Lamanna, Caputo, Di Gennaro, Lefons and Riccio (2013)]. Experimental activities, aimed to characterize the damage in terms of matrix and fibers breakage in laminated composites, are presented by Allix and Blanchard (2006). Often, from an experimental point of view, fiber and matrix cracking in composites have been found strongly related to the delamination onset and growth events [Sharif-Khodaei, Ghajari and Aliabadi (2012)]. From an analytical and numerical point of view, the progression of damage in composites in term of matrix and fiber failure is the subject of several papers. The failure criteria and the material properties degradation rules are identified as the basic steps for a progressive damage approach in composite structures. In order to take into account the degradation of the material properties on failure occurrence, several material degradation models are available in literature. Three categories for the material degradation models can be identified: instantaneous unloading [Murray and Schwer (1990)], gradual unloading [Petit and Waddoups (1969)] and constant stress at ply failure [Nahas (1986)]. However none of the previously cited research works deals with the interactions between delamination and matrix-fiber damage mechanism in laminated composites under any loading conditions. These interactions can have a relevant role in particular for delaminated composite plates under impact loading, compression loading or compression after impact loading. Hence, for the simulation of the complex physical phenomena behind the impact and/or compressive behavior of delaminated plates, the development of integrated numerical methodologies considering simultaneously the presence of different damage mechanisms in composites becomes mandatory. The aim of this work is to develop, through a numerical-experimental correlation,

a modeling and a simulating technique for a Low Velocity Impact event involving a laminate composite structure.

2 Description of composite failure mechanisms

There are different types of damages interesting composite structure: the breaking of the fibers, the progressive damage in the matrix (matrix cracking), the interface damage between fibers and matrix (debonding) and the stress concentration around a crack [Caputo, Lamanna and Soprano (2006, 2011, 2012-3, 2013-2)]. In this case the damages are often caused by in-plane layer stresses. Another type of damage is the delamination between different layers. This damage is caused by the interlaminar out of plane stress components [Lekhnitskii (1968); Hashin (1980); Ferencz (1989); Johnson and Cook (1985); Liu (1988)]. The damage mechanisms can evolve independently, or may interact with each other.

In the present paper, the ply failure is modeled within the Abaqus Explicit Solver® by considering Progressive Damage of Fiber-Reinforced Composites technique, while the delamination failure is modeled by using the cohesive elements technique [Spilker, Verbiese, Orringer, French, Witmer and Harris (1976)]. The following subsections describe the two different numerical techniques.

2.1 Progressive damage modeling

The progressive Damage technique implemented in the Abaqus® code offers a general capability of modeling progressive damage and failure in fiber-reinforced composites.

Four different modes of failure are considered, which are fiber rupture in tension and compression, and matrix cracking under transverse tension and compression. In Figure 1 the constitutive law modeling the progressive failure of a finite element is shown.

The undamaged constitutive behavior is defined as orthotropic elastic. The Fiber-Reinforced Composite damage model combines an initialization phase and a propagation phase. When the element stress exceeds a limit value, the element is considered partially damaged and the damage propagation starts.

The point A in Figure 1 shows the damage initiation followed by the material stiffness degradation. The damage initiation criteria for fiber reinforced composites are based on Hashin's theory (Hashin (1980)]. In Table 1, the Hashin's failure criteria are summarized.

The path A-B shows the damage evolution that defines the post damage-initiation material behavior. It describes the rate of degradation of the material stiffness once the initiation failure criterion is satisfied. For the damage propagation, a linear
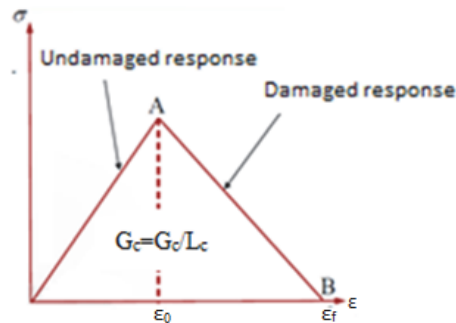
Figure 1: The damage definition of the material

evolution law has been considered. This law is based on the energy dissipated during the process. A linear material stiffness softening is assumed. In particular, the damage evolution considers the longitudinal and transverse fracture energies. By default, an element is removed (deleted) once the damage parameters for all the failure modes at all material points in the element reach the value "Dmax" (max degradation). The damage evolution based on fracture energy is also used in cohesive element modeling approach that is described in the next sub-sections.

Table 1: Hashin's failure criteria

Hashin's Failure criteria	
$\left(\frac{\sigma_{11}}{X_t}\right)^2 + \alpha\left(\frac{\tau_{12}}{S_l}\right)^2 = 1$	Fiber Tensile failure
$\left(\frac{\sigma_{11}}{X_c}\right)^2 = 1$	Fiber Compressive failure
$\left(\frac{\sigma_{22}}{Y_t}\right)^2 + \left(\frac{\tau_{12}}{S_l}\right)^2 = 1$	Matrix Tensile failure
$\left(\frac{\sigma_{22}}{2S_t}\right)^2 + \left[\left(\frac{Y_t}{2S_t}\right)^2 - 1\right]\left(\frac{\sigma_{22}}{Y_t}\right)^2 + \left(\frac{\tau_{12}}{S_l}\right)^2 = 1$	Matrix Compressive failure

2.2   *Interlaminar Damage*

In order to capture the phenomena of delamination, special finite elements have been used, the cohesive elements, which aim at reproducing correctly the characteristics of stiffness, strength and fracture toughness of the interface between different layers.

The main advantage that these elements provide consists in the ability to predict

both the initiation and the propagation of delamination defect, without any knowledge of the initial position of the crack and of the direction of propagation [Caputo, Lamanna, Lanzillo and Soprano (2013)].

The cohesive element is an element based on the theory of continuous with reduced thickness and it is used to simulate situations where the thickness of bonding is much lower than that of the elements in contact, as happens in composite laminates.

The mechanical response of the cohesive element is described through a constitutive load relating the interlamina stress to the separation displacement between the nodes linked via cohesive element (Figure 2). With increasing interfacial separation, the traction across the interface reaches a maximum, decreases and eventually vanishes so that complete decohesion occurs. Hence, the constitutive response in cohesive elements for delamination modeling is characterized by an initial damage phase, a damage evolution phase and the possibility to remove full damaged elements.

The cohesive damage evolution is usually based on two types of criteria. The first one is an energy criterion, the second one is a displacement criterion. Therefore, the total fracture energy must be specified when the energy criterion is used, while the post-damage ultimate displacement at failure of the element must be defined for displacement criterion. The fracture energy is defined as the area under the constitutive response curve [Puck and Schürmann (2001)].

In this work the damage evolution based on fracture energy has been used.

In the graph of Figure 2, relative to the considered constitutive law, it is possible to distinguish the two areas in which the element shows different behaviors: in the first zone, where there is still contact between the surfaces, the tension in the element increases linearly with the relative displacement the slope of the straight line is equal to Kp, a penalty stiffness value; in the second zone, that is when the relative displacement become greater than the displaceement $\delta_{0,I}$, the reaction of the cohesive decreases with increasing displacement.

The force exerted by the element decreases to zero for a limit value of displacement $\delta_{max,I}$ for the i-th mode of fracture.

3 Validation analysis

The problem used as reference case in order to validate the proposed numerical methodology consists of a Low Velocity Impact (LVI) on a composite plate specimen according to the ASTM D7136 (American Standard Test Method for Measuring the Damage Resistance of a Fiber –Reinforced Polymer Matrix Composite to a Drop-Weight Impact) regulations. Generally, LVIs produce interlaminar and intralaminar damage which can significantly reduce the load capability of the plate.
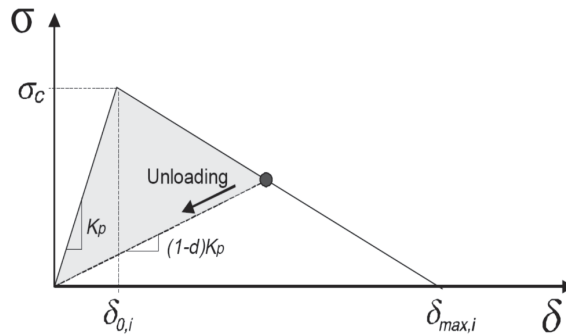
Figure 2: Bilinear cohesive constitutive law

According to the above mentioned standard test, the plate is impacted by a rigid hemispherical body with a fixed kinetic energy value.

3.1   Test case description

The experimental data of the impact test were developed at CIRA (Centro Italiano Ricerche Aerospaziali) laboratories. The test is a simple LVI on a clamped composite plate specimen made of CFRP composed by 24 plies $[(45,-45,0,90)_3]_{sym}$. The specimen is impacted by a steel hemispherical impactor with a diameter of 20 mm and a mass of 7.5 Kg. The drop height is chosen in order to obtain the desired impact velocity and impact energy. In this work, impact tests were performed at 50 J and 100 J. The global plate thickness is 4.3 mm where each ply is 0.179 mm thick. A comprehensive material characterization test campaign was carried out before the impact tests. In Table 2 the material properties of the unidirectional lamina are summarized.

3.2   FE Model

A Global-Local approach has been used to model the composite plate specimen: a refined mesh in the impact zone has been adopted and a coarser one has been considered in the rest of the model [Sellitto, Borrelli, Caputo, Riccio, and Scaramuzzino (2012)]. This technique allows reducing the required CPU time. In the impact zone, each composite ply has been modeled with one layer of finite element. Furthermore, between two layers, cohesive elements have been placed to simulate the ply bonding.

Since the plate is composed by 24 plies, 23 layers of cohesive elements have been used. The thickness of cohesive elements is 0.001 mm.

Table 2: Material Properties

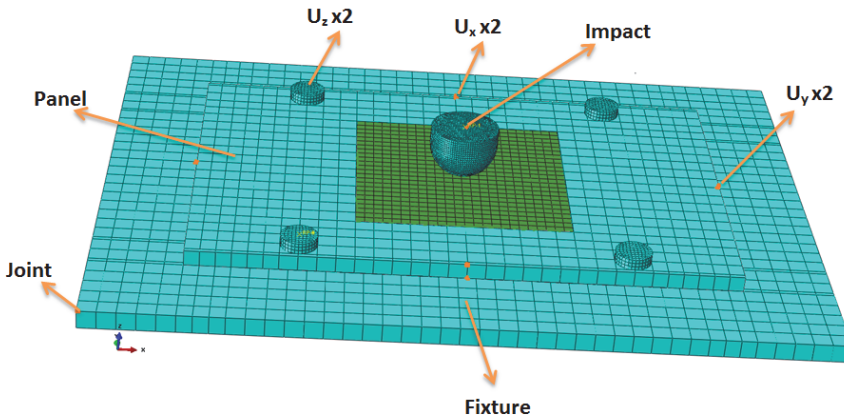| Longitudinal Young's Modulus E_{11}	156	GPa
Transverse Young's Modulus E_{22}	8.35	GPa
In Plane Shear Modulus $G_{12} = G_{13}$	4.2	GPa
In Plane Shear Modulus G_{23}	2.52	GPa
Poisson's ratio $v_{12=}v_{13}$	0.33	
Poisson's ratio v_{23}	0.55	
Critical ERR-MODE G_{IC}	288	Jm^{-2}
Longitudinal Tensile Strenght X_t	2500	MPa
Longitudinal Compressive Strenght Xc	1400	MPa
Transverse Tensile Strenght Yt=Zt	75	MPa
Transverse Compressive Strenght Yc=Zc	250	MPa
Shear Strenght $S_{12}=S_{13}$	95	MPa
Shear Strenght S_{23}	108	MPa
Critical ERR-MODE II-III $G_{II-IIIc}$	610	Jm^{-2}

Figure 3: Boundary conditions

The Shell Continuum (SC8R) and Cohesive (COH3D8) elements have been select-ed from the Abaqus element library. Algorithms of dynamic explicit analyses have been used [Gallo and Piccirillo (2012)], by enabling the removal element capabil-ity. The tup has been modeled as a rigid body, with mass and velocity values able to simulate the real test conditions. In Figure 3 the FE boundary conditions are shown.

The local zone is linked with the global zone via "tie constraints" elements, chosen from the ABAQUS elements' library. This technique allows linking all degrees of freedom of a geometrical surface to another surface. In this case the node to surface contact is used improving numerical convergence of results. Two different methods are available for modelling composites with both continuum shell and cohesive elements: using a coincident or not coincident mesh (Figure 4).
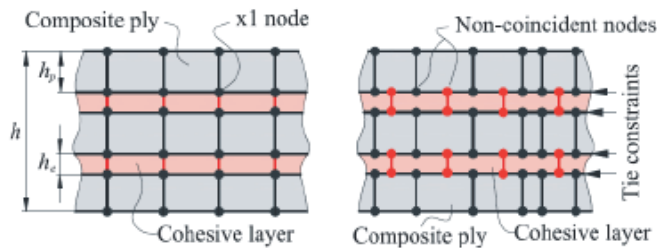

Figure 4: Different strategies for modelling composites

A coincident mesh between the cohesive and composite layer makes the model simpler and less computationally expensive (no use of tie constrains), but the necessity to have a very fine mesh in the cohesive layers leads to have too muchsmall elements in the model.

By using not coincident meshes, the possibility to locally change the elements sizes allows for optimization of the element's dimensions and consequently the dimension of the total model. This technique is more complex and makes the pre-processing phase more laborious, but in some cases it may allow to save computational time. All the FE models presented here have been prepared by using the coincident mesh strategy.

3.3   FE Results and Numerical-Experimental Correlation

The FE model described above has been used to simulate both impact experimental tests, at energy value of 50 J and of 100 J. In the Figures 5 and 6 the numerical results for the test case at 50 J are compared to the experimental ones. In particular the impactor force (Figure 5a), the absorbed energy (Figure 5b), the impactor displacement (Figure 6a) and the impactor velocity (Figure 6b) are plotted as function of the time.

As expected, the impact force increases with the increasing of impact energy producing more damage [Ghajari, Sharif-Khodaei, Aliabadi, and Apicella (2013)]. The force increases almost linearly up to about 8000 N where a first sudden force

drop, indicating the onset of the first damage, can be appreciated. Further force drops are registered successively due to the damage propagation.

The numerical force curve has been found in a good agreement with the experimental results. As matter of the fact, the first ply failure load, the maximum impact force and the duration of the impact event are reproduced accurately. Also, the maximum displacement predicted by the FE model is in agreement with the experimental one. The energy absorbed by the plate is slightly underestimated and for this reason the numerical impactor final velocity (1.85 m/s) is greater than the experimental value (0.8 m/s).
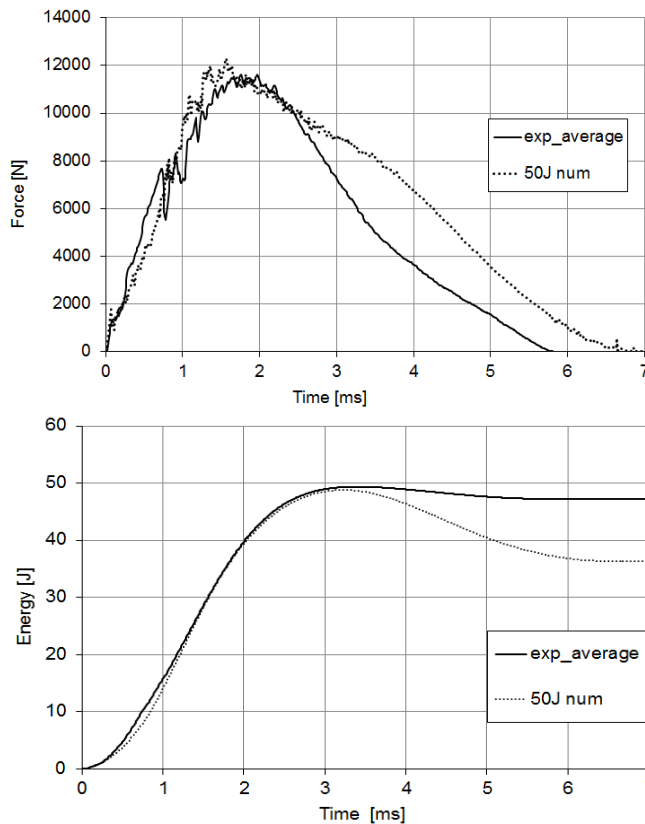
Figure 5: Force vs Time (a); Energy vs Time (b)

In the Figure 7 the numerical results of the interlaminar damage associated with the failed cohesive element are shown.

In Figure 8, the force vs. displacement numerical curve is reported. The envelope
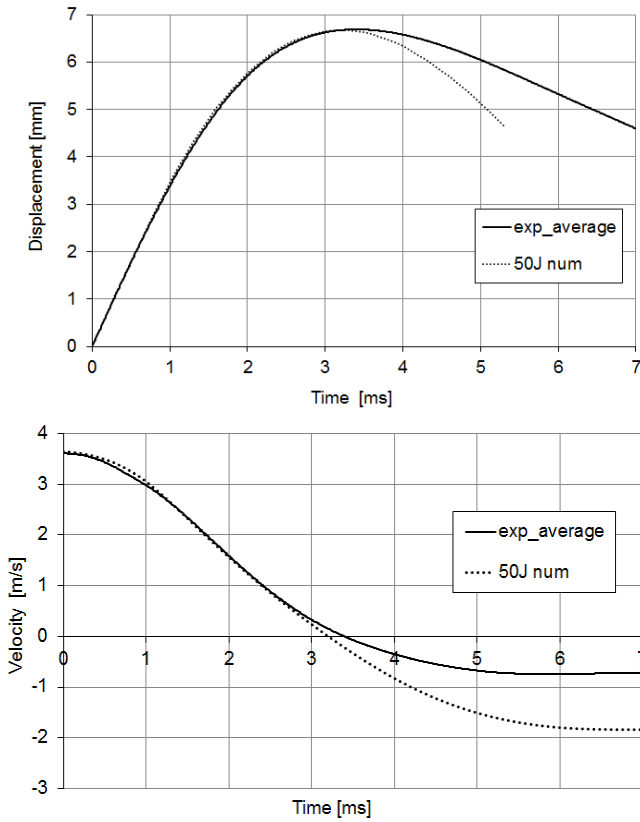
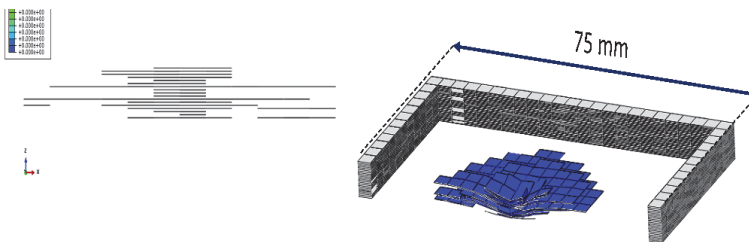Figure 6: Displacement Impactor vs Time (a); Velocity vs Time (b)

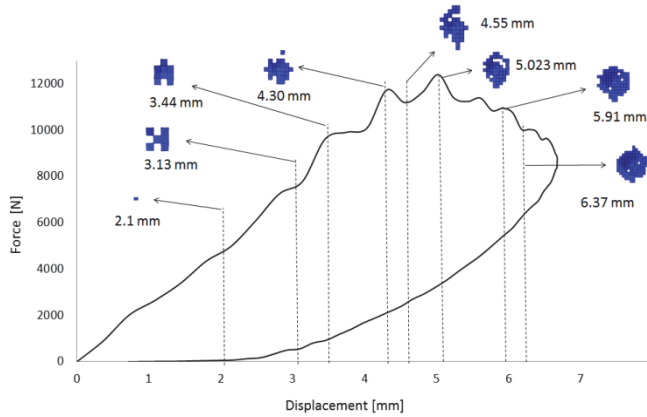Figure 7: Envelope Delamination (Energy Impact 50 J)

Figure 8: Force vs. Displacement Curve (Energy Impact 50J)

Table 3: Comparison between numerical and experimental value

Impact 50J	Numerical Values	Average experim. values	Percentage change
Delamination	750 mm^2	1095,67 mm^2	- 31.54%
Displacement	6.67 mm	6.69 mm	- 0.29%
Force	12300 N	11603 N	+ 6.0%

Table 4: Comparison between numerical and experimental data for the 100J impact test

Impact 100J	Numerical Values	Average experim. values	Percentage change
Delamination	2025 mm^2	1880,67 mm^2	+ 7.67%
Displacement	10.6 mm	10.63 mm	- 0.28%
Force	14300	12898	+ 10.86%

of failed cohesive elements is also shown at different time in order to have an idea about the progression of the intralaminar damage. It can be noted that after reaching the peak force, the delamination continues to increase and reaches its final shape close to the point of maximum displacement.

In Table 3 and 4 it is shown the comparison between the numerical and experimental data in terms of delaminated area extension, maximum displacement and peak value of the impact force respectively for the 50J and 100J tests. The estension

of the damaged area has been measured experimentally by means of ultrasonic C-scan. As mentioned above, a good agreement has been found for the peak force and peak displacement. The damaged area is underestimated and this reflects the underestimation of the absorbed energy.

4   Conclusions

Numerical studies for the structural analysis of a composite plate subjected to low velocity impact have been carried out. The described methodology is appropriate for the simultaneous study of the interlaminar and intralaminar damage in the composite structure and has been validated against experimental standard impact test results.

These numerical studies have provided very interesting results regarding Low Velocity Impact damaging mechanism of a composite plate. The considered numerical techniques allow estimating damages in good agreement with experimental results.

The failure criteria modeling technique allowed predicting delamination growth (cohesive element criterion) and fiber and matrix failure (maximum stress criterion). A Global-Local modeling Approach has been used to model the plate specimen, gaining CPU time.

The development and validation of these techniques lead to a significant benefit in the industry especially in the certification process.

References

Allix, O.; Blanchard, L. (2006): Mesomodelling of Delamination: Towards Industrial Applications. *Compos Sci Technol*, vol. 66, pp. 731-744.

Armentani, A.; Caputo, F.; Esposito, R.; Godono, G. (2004): Evaluation of energy release rate for delamination defects at the skin/stringer interface of a stiffenedcomposite panel. *Eng Fract Mech*, vol. 71/4-6, pp 885-895.

Armentani, E.; Calì, C.; Caputo, F.; Cricrì, G.; Esposito, R. (2006): Numerical solution techniques for structural instability problems. *Journal of Achievements in Materials and Manufacturing Engineering*, vol. 19, pp. 53-64.

Backman, M. E.; Goldsmith, W. (1978): The Mechanics of Penetration of Projectiles into Targets. *Int J Eng Sci*, vol. 16, pp. 1-91.

Caputo, F.; Esposito, R.; Perugini, P.; Santoro, D. (2002): Numerical-experimental investigation on post-buckled stiffened composite panels. *Compos Struct*, vol. 55 (3), pp. 347-357.

Caputo, F.; Lamanna, G.; Lanzillo, L.; Soprano, A. (2013): Numerical inves-

tigation on LEFM limits under LSY conditions. *Key Eng Mat*, vol. 577-578, pp. 381-384.

Caputo, F.; Lamanna, G.; Soprano, A. (2006): Numerical Investigation on the Crack Propagation in a Flat Stiffened Panel. *Key Eng Mat*, vol. 324-325, pp. 559-562.

Caputo, F.; Lamanna, G.; Soprano, A. (2013): Residual strength improvement of an aluminium alloy cracked panel. *The Open Mechanical Engineering Journal*, vol. 7, pp. 88-95.

Caputo, F.; Lamanna, G.; Soprano, A. (2013): On the evaluation of the plastic zone size at the crack tip. *Eng Fract Mech*, vol. 103, pp. 162-173.

Caputo, F.; Lamanna, G.; Soprano, A. (2011): An analytical formulation for the plastic deformation at the tip of short cracks. *Procedia Engineering*, vol. 10, pp. 2988-2993.

Caputo, F.; Lamanna, G.; Soprano, A. (2012): Handling of composite-metal interface in a hybrid mechanical coupling. *AIP Conf Proc,* vol. 1459, pp. 353-355.

Caputo, F.; Lamanna, G.; Soprano, A. (2012): Geometrical parameters influencing a hybrid mechanical coupling. *Key Eng Mat*, vol. 525-526, pp. 161-164.

Caputo, F.; Lamanna, G.; Soprano, A. (2012): Effects of Tolerances on the Structural Behavior of a Bolted Hybrid Joint. *Key Eng Mat*, vol. 488-489, pp. 565-569.

Chai, H.; Babcock, C. D.; Knauss, W. G. (1981): One dimensional modelling of failure in laminated plates by delamination buckling. *Int J Solids Struct*, vol. 17, pp. 1069-1083.

De Angelis, G.; Caputo, F.; Lamanna, G.; Pannullo, F. M. (2012): A Methodological Approach to the Tolerance Problems during the Assembly Process of Deformable Bodies. *Key Eng Mat*, vol. 488-489, pp. 557-560.

Fei, Z.; Yin, W. L. (1984): Postbuckling Growth of a Circular Delamination in a Laminate Under Compression and Bending. *Proc. of the Twelfth South-eastern Conf. on Theoretical and Applied Mechanics, Georgia Inst. Of Technology, Pine Mountain, Georgia*.

Ferencz, R. M. (1989): Element-by-Element Preconditioning Techniques for Large-Scale, Vectorized Finite Element Analysis in Nonlinear Solid and Structural Mechanics, Ph. D. Dissertation. *Stanford University, Stanford*, CA.

Gallo, A.; Piccirillo, A. M. (2012): Multidimensional impulse inequalities and general binari type inequalities for discontinuous functions with delay. *Nonlinear Studies*, vol. 19 (1), pp. 115-126.

Gallo, A.; Piccirillo, A. M. (2012): New Wendroff's type inequalities for discon-

tinuous functions and its applications. *Nonlinear Studies*, vol. 19, pp. 1-11.

Ghajari, M.; Sharif-Khodaei, Z.; Aliabadi, M. H.; Apicella, A. (2013): Identification of impact force for smart composite stiffened panels. *Smart Mater. Struct.* vol. 22, 085014.

Hashin, Z. (1980): Failure criteria for unidirectional fiber composites. *J Appl Mech-T Asme*, vol. 47, pp. 329-334.

Johnson, G. R.; Cook, W. H. (1985): Fracture Characteristics of Three Metals Subjected to Various Strains, Strain rates, Temperatures and Pressures. *Eng Fract Mech*, vol. 21, no. 1, pp. 31-48.

Karan, S. S.; Sorem, R. M. (1990): Curved Shell Elements Based on Hierarchical-Approximation in the Thickness Direction for Linear Static Analysis of Laminated Composites. *Int J Numer Meth Eng*, vol. 29, pp. 1391-1420.

Kardomates, G. A.; Schmueser, D. W. (1988): Buckling and post-buckling of delaminated composites under compressive loads including transverse shear effects, *AIAA J*, vol. 27, pp. 337-343.

Lamanna, G.; Caputo, F.; Di Gennaro, F.; Lefons, A.; Riccio, A. (2013): Numerical procedures for damage mechanisms analysis in CFRP composites. *Key Eng Mat*, vol. 569-570, pp. 111-118.

Lekhnitskii, S. G. (1968): Anisotropic Plates, translated from second Russian edition by S. W. Tsai and T. Cheron, Gordon and Breach, New York.

Liu, D. (1988): Impact induced delamination - a view of bending stiffness mismatching. *J Compos Mater*, vol. 22 (7), pp.674-692.

Murray, Y.; Schwer, L. (1990): Implementation and Verification of Fiber-Composite Damage Models. Failure Criteria and Analysis in Dynamic Response. *ASME AMD*, vol. 107, pp. 21-30.

Nahas, M. N. (1986): Survey of Failure and Post-Failure Theories of Laminated Fiber-Reinforced Composites. *J Compos Tech Res*, vol. 8, pp. 138-153.

Nilsson, K. F.; Thesken, J. C.; Sindelar, P.; Giannakopoulos, A. E.; Storakers B. (1993): A Theoretical and Experimental Investigation of Buckling Induced Delamination Growth. *J Mech Phys Solids*, vol. 41, no. 4, pp. 749-782.

Petit, P. H.; Waddoups, M. E. (1969): A Method of Predicting the Non-linear Behavior of Laminated Composites. *J Compos Mater*, vol. 3, pp. 2-19.

Puck, A.; Kopp, J. (2001): Guidelines for the determination of the parameters in Puck's action plane strength criterion. *Compos Sci Technol*, vol. 62, no. 3, pp. 371-378.

Puck, A.; Schürmann, H. (2001): Failure analysis of FRP laminates by means

of physically based phenomenological models. *Compos Sci Technol*, vol. 62 no. 12-13, pp. 1633-1662.

Riccio, A.; Caputo, F.; Tessitore, N. (2013) Intra-laminar Damage Evolution in a Composite Grid Structure Representative Volume Element under Compression Load. *Structural Durability and Health Monitoring*, vol. 9, no. 1, pp. 43-66.

Riccio, A.; Zarrelli, M.; Caputo, F. (2013): Damage Propagation in Composite Structure using an Embedded Global-Local Approach. *Structural Durability and Health Monitoring*, vol. 9, no. 1, pp. 21-41.

Sellitto, A.; Borrelli, R.; Caputo, F.; Riccio, A.; Scaramuzzino, F. (2012): Application of the Mesh Superposition Technique to the Study of Delaminations in Composites Thin Plates. *Key Eng Mat*, vol. 525-526, pp. 533-536.

Sellitto, A.; Borrelli, R.; Caputo, F.; Riccio, A.; Scaramuzzino, F. (2012): Application to plate components of a kinematic global-local approach for non-matching Finite Element meshes. *International Journal of Structural Integrity*, vol. 3, no. 3, pp. 260-273.

Sharif-Khodaei, Z.; Ghajari, M.; Aliabadi, M. H. (2012): Determination of impact location on composite stiffened panels. *Smart Mater. Struct.* vol. 21, 105026.

Spilker, R. L.; Verbiese, O.; Orringer, S. E.; French, E. A.; Witmer, A.; Harris, A. (1976): Use of the Hybrid-Stress Finite-Element Model for the Static and Dynamic Analysis of Multilayer Composite Plates and Shells. *Report for the Army Materials and Mechanics Research Center*, Watertown, MA.

Whitcomb, J. D. (1986): Parametric Analytical Study of Instability-Related Delamination Growth. *Compos Sci Technol*, vol. 25, no. 1, pp. 18-48.